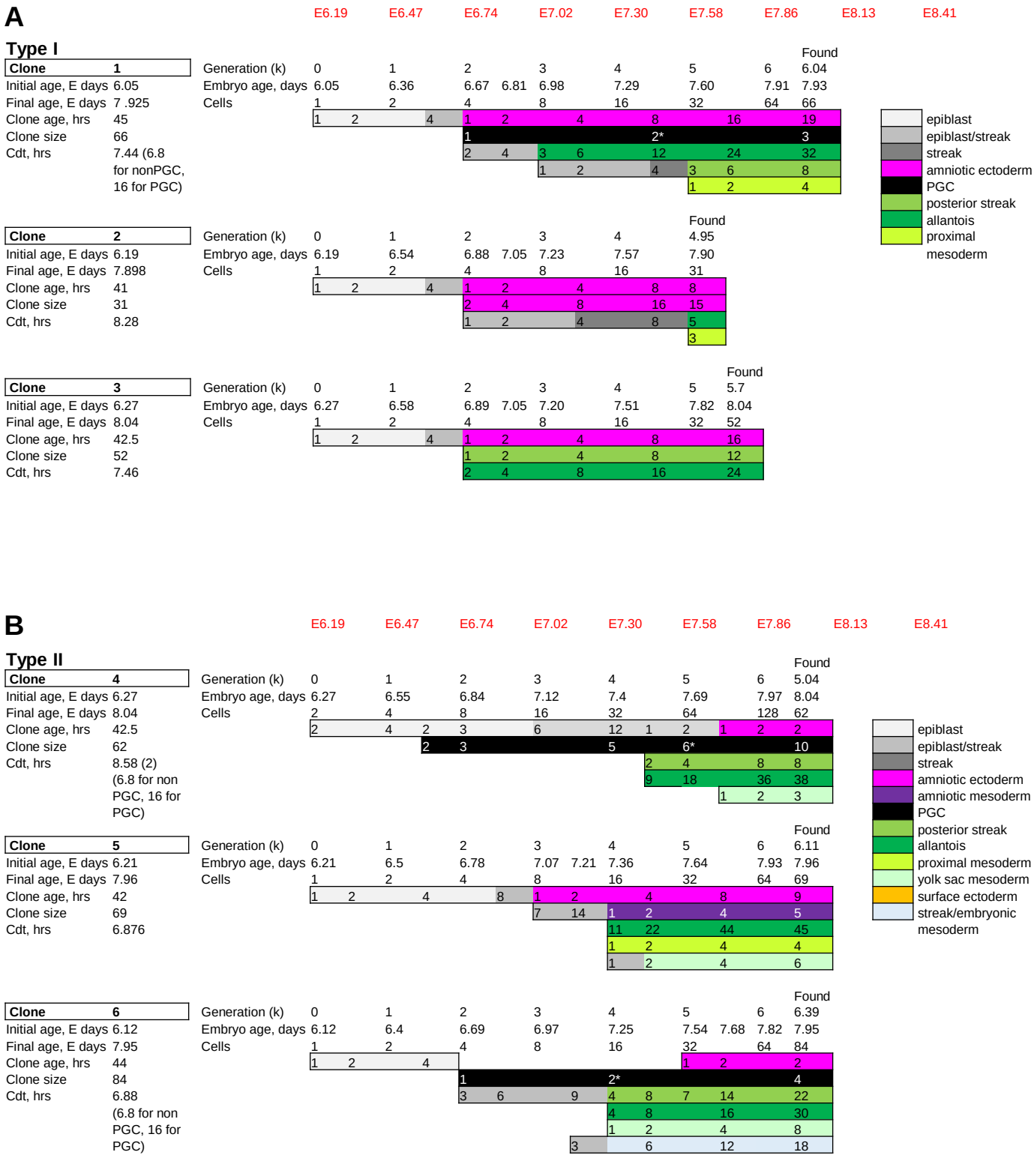

B (continued)

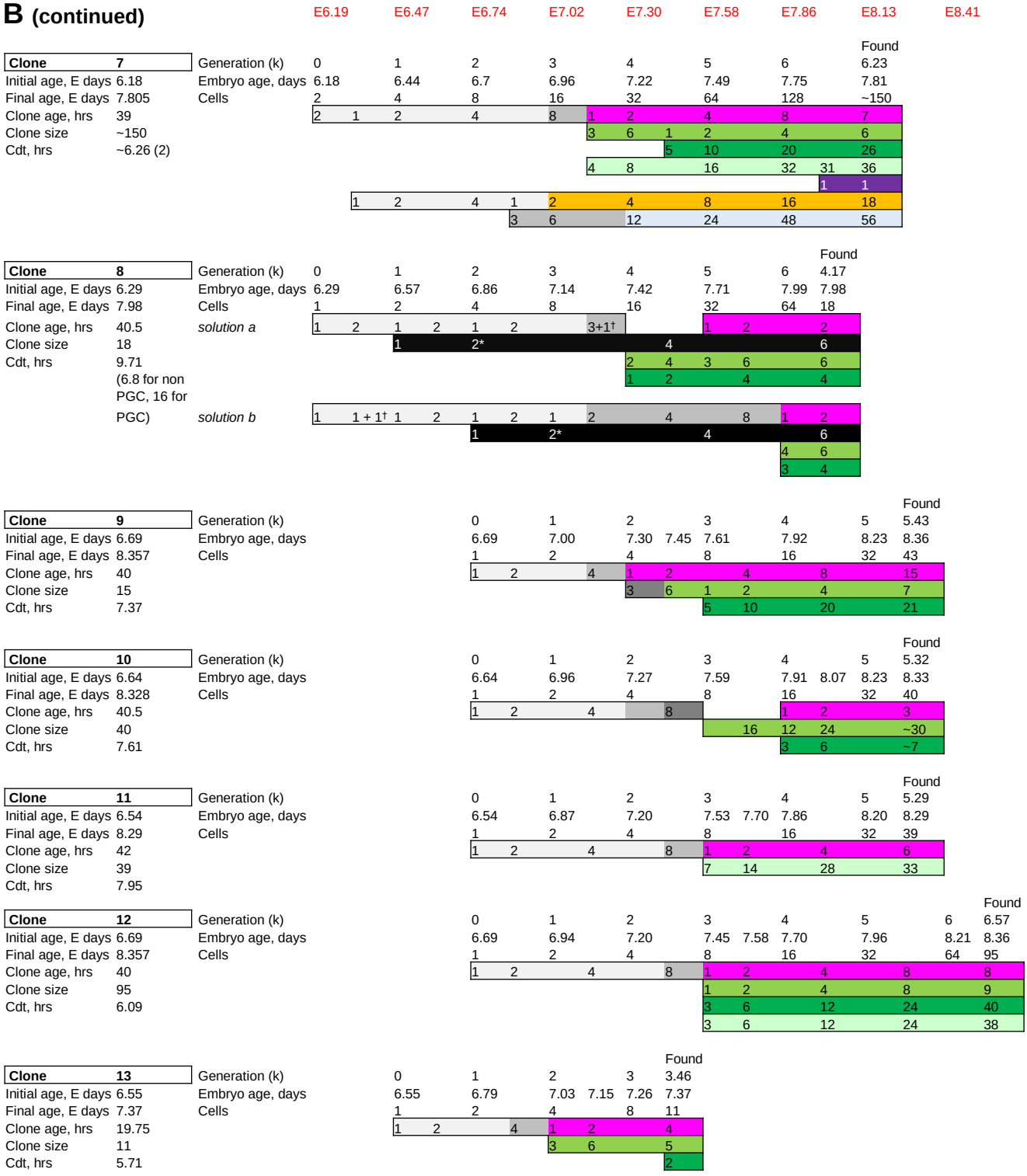

B (continued)

E6.19 E6.47 E6.74 E7.02 E7.30 E7.58 E7.86 E8.13 E8.41

Clone	**14**	Generation (k)	0	1	2	3	4	5	Found 5.64
Initial age, E days	6.59	Embryo age, days	6.59	6.89	7.20	7.50	7.8	8.10	8.30
Final age, E days	8.298	Cells	2	4	8	16	32	64	~100
Clone age, hrs	41		2	4	8	16		1	2 2
Clone size	~100						3	6 5	10 13
Cdt, hrs	7.26 (2)						13	26	52 85

Clone	**15**	Generation (k)	0	1	2	3	4	Found 4.17
Initial age, E days	6.71	Embryo age, days	6.71	6.94	7.16	7.39 7.50	7.61	7.65
Final age, E days	7.648	Cells	1	2	4	8	16	18
Clone age, hrs	22.5		1 2	4	8	1	2	2
Clone size	18					4	8	9
Cdt, hrs	5.4					3	6	7

C

E6.19 E6.47 E6.74 E7.02 E7.30 E7.58 E7.86 E8.13 E8.41

Type III

Clone	**16**	Generation (k)	0	1	2	3	4	Found 4.13
Initial age, E days	6.65	Embryo age, days	6.65	6.90	7.14	7.39	7.63	7.67
Final age, E days	7 .67	Cells	2	4	8	16	32	35
Clone age, hrs	24.5		2	4	8	7 14	1+1 2+2	4
Clone size	35						12 24	1
Cdt, hrs	5.93 (2)							23
						1 2	4	6

Clone	**17**	Generation (k)	0	1	2	3	4	Found 4.95
Initial age, E days	6.5	Embryo age, days	6.5	6.84	7.17 7.34	7.51	7.84	8.17
Final age, E days	8.167	Cells	1	2	4	8	16	31
Clone age, hrs	40		1 2	4	1 2	4		8
Clone size	31				3 6	12		23
Cdt, hrs	8.07							

Clone	**18**	Generation (k)	0	1	2	3	Found 3.32
Initial age, E days	6.85	Embryo age, days	6.85	7.11	7.38 7.51	7.64	7.73
Final age, E days	7.725	Cells	1	2	4	8	10
Clone age, hrs	21		1 2	4	1	2	2
Clone size	10				3	6	8
Cdt, hrs	6.32						

Clone	**19**	Generation (k)	0	1	2	3	4	Found 4.75
Initial age, E days	6.88	Embryo age, days	6.88	7.21	7.54 7.70	7.87	8.12	8.44
Final age, E days	8.443	Cells	1	2	4	8	16	27
Clone age, hrs	37.5		1 2	4	1	2	4	5
Clone size	27				3	6	12	22
Cdt, hrs	7.89							

Clone	**20**	Generation (k)	0	1	2	3	4	5	6	Found 6.19
Initial age, E days	6.57	Embryo age, days	6.57	6.85	7.13	7.41 7.55	7.69	7.97	8.24	8.30
Final age, E days	8.299	Cells	1	2	4	8	16	32	64	73
Clone age, hrs	41.5		1 2	4	8	1 2	4	8		10
Clone size	73					7 14	13	26	52	57
Cdt, hrs	6.7						1	2	4	6

Clone	**21**	Generation (k)	0	1	2	3	4	5	6	Found 6.95
Initial age, E days	6.48	Embryo age, days	6.48	6.74	6.99	7.25	7.50	7.76	8.02	8.26
Final age, E days	8.26	Cells	2	4	8	16	32	64	128	~250
Clone age, hrs	42.75		2	4	8	16	1 2	4	8	14
Clone size	~250						15 30	25 50	100	~197
Cdt, hrs	6.14 (2)							5 10	7 14	~27
									3 6	12

Clone	**22**	Generation (k)	0	1	2	3	4	5	Found 5.46
Initial age, E days	6.67	Embryo age, days	6.67	6.98	7.29 7.44	7.60	7.91	8.22	8.36
Final age, E days	8.358	Cells	1	2	4	8	16	32	44
Clone age, hrs	40.5		1 2	4	1	2	4	8	8
Clone size	44				2	4	8	16	27
Cdt, hrs	7.42				1	2	4	8	9

epiblast
epiblast/streak
streak
amniotic ectoderm
posterior streak
allantois
surface ectoderm
distal half embr.
ectoderm

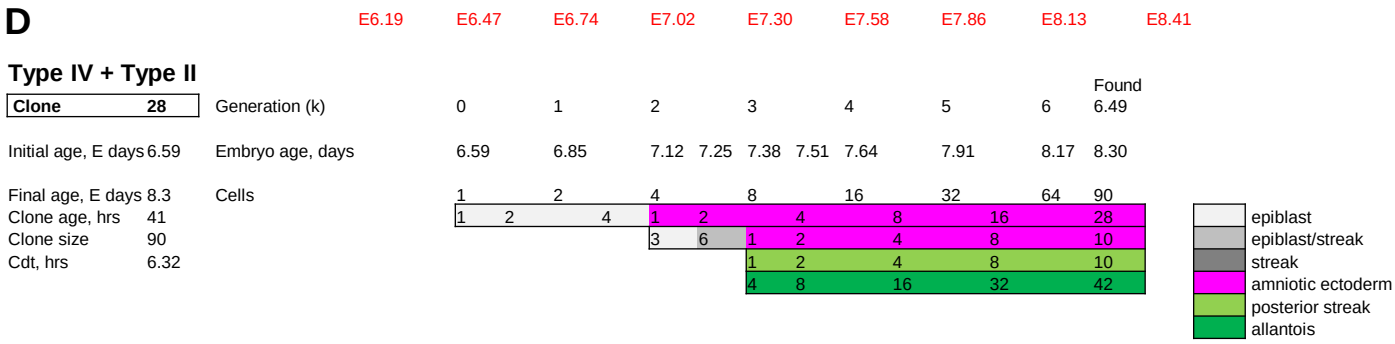

Figure S1. Inferred clonal histories of clones contributing to amniotic ectoderm.
Histories of: (**A**) Type I, (**B**) Type II, (**C**) Type III and (**D**) Type IV + Type II are shown.

1. Exponential growth is assumed. Then $N = a.e^{bt}$, or $\ln N_t = \ln N_0 + bt$, where N_t is final clone size, N_0 is initial clone size (usually 1, but 2 when siblings still joined by a cytoplasmic bridge were labelled), t is clone age. Clone doubling time (Cdt) is $\ln 2 / b = \ln 2 \times t / \ln N_t - \ln N_0$. The number of cell generations (k) is derived from $2^k = N_t / N_0$, then $k = \ln N_t - \ln N_0 / \ln 2$.
2. When estimating the distribution of cell generations, the first generation is expected to be shortened because the likelihood of impaling a columnar cell associated with the basement membrane and near the middle of the cell cycle is greater than impaling a mitotic or early post-mitotic one at the lumen (Gardner and Cockroft, 1998). When 2 siblings are initially labelled, the first generation is assumed to require a whole cell cycle.
3. No evidence for any significant difference in cell cycle length within the proximal half of the epiblast between E6 and E8 has been found (Lawson et al., 1991; Tzouanacou et al., 2009) except for the PGCs. The contribution to PGCs in clones 1, 4, 6 and 8 was calculated according to (Lawson and Hage, 1994), modified to accommodate cell cycle lengthening during specification (McLaren and Lawson, 2005) until the PGC founding population closed at allocation (*).
4. In mixed clones, the calculated generation of entry into the amniotic ectoderm is supported by the ‘found’ distribution of the rest of the clone, although the intermediate distribution of the latter will be speculative if intermediate generations have transited through the streak, and possibly other regions. In contrast, the time of transition of pure clones from the epiblast to the amniotic ectoderm cannot be formally obtained: therefore no clonal histories are provided for Type IV clones that contributed exclusively to amniotic ectoderm.
5. Clonal data: The distribution of descendants ‘found’ is shown in the last column of Table 1 with its 8 subcolumns (“Clone distribution”). Differences from the calculated distribution at the last whole generation include natural variation (e.g. loss of cell cycle synchrony, apoptosis) and counting errors, as well as the difference between the final age of the clone and the calculated number of completed generations. Separation to a new cell category is made in the earliest possible cell generation, but does not exclude separation being made later by descendants. The estimate of the age at which the first cell in the amniotic ectoderm would have divided is used for comparison within and between clone types (see main text). Clone 8 has two possible solutions: one cell death (†) is assumed in order to account for the low number of somatic cells found (12) compared with expected (16 in solution a, 32 or 40 in solution b). E days (top row, in red) are a guide for the rough alignment of the clonal histories: they are based on the Cdts of the displayed clones with a start time from the E6.2 group.

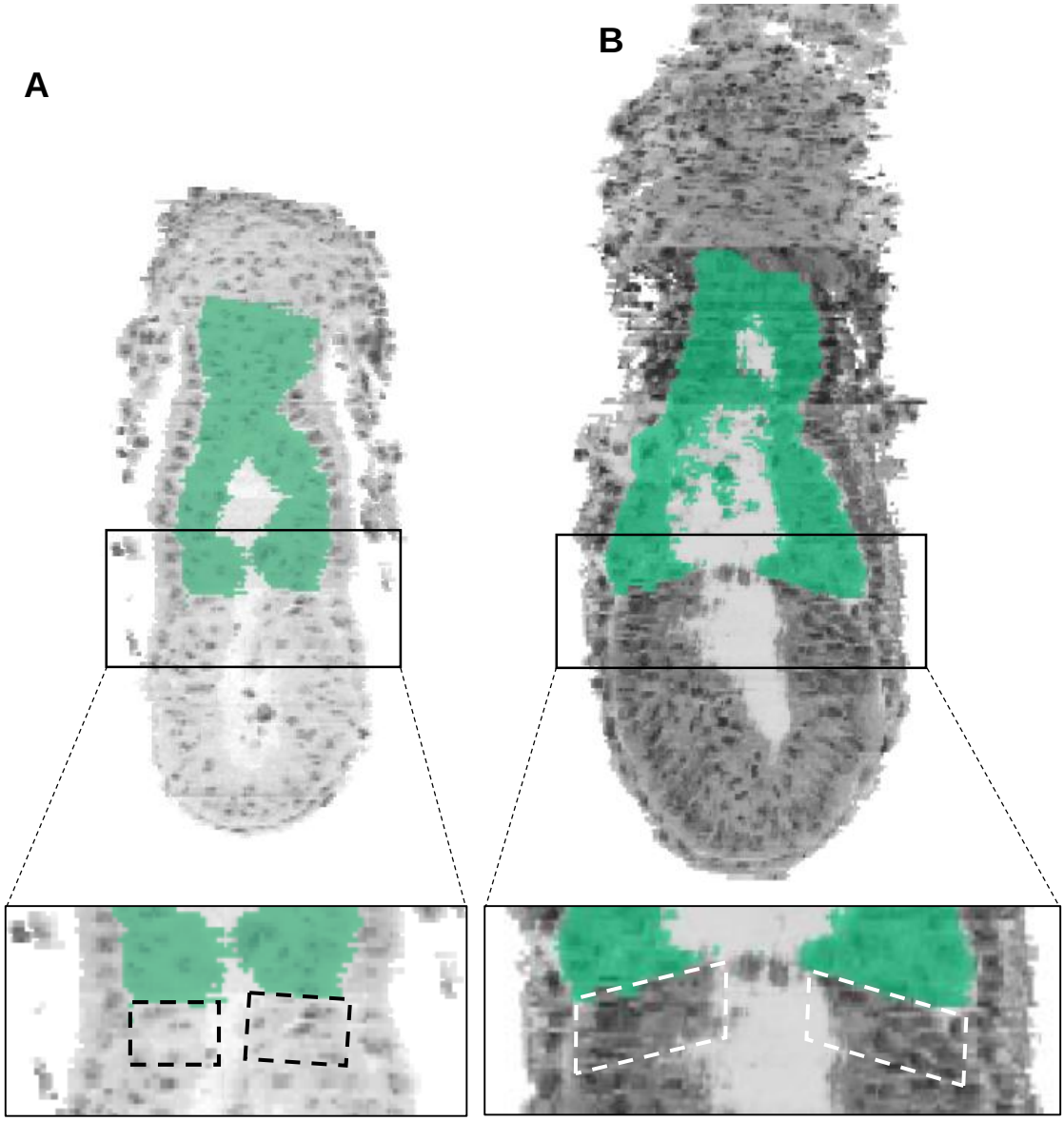

Figure S2. Possible explanation for the absence of Type I clones of amniotic ectoderm after injection at ES.

The cellular conformation at the embryonic-extraembryonic interface differs between PS (A) and ES (B) stages of development. At the ES stage (B), junctional anterolateral epiblast cells appear compressed and the interface tilts proximally towards the proamniotic cavity. The extraembryonic ectoderm is painted green. Images of frontal slices through embryo reconstructions reproduced from e-MouseAtlas (http://www.emouseatlas.org/emap/ema/home/.php) (Armit et al., 2017). A: EMA:8: TS8 (frontal:: pitch 90, yaw 257, roll 90, d 0), B: EMA:9: TS9 (frontal: pitch 94, yaw 69, roll 90, d -16).

Either conformational difference would reduce the chance of successfully injecting an epiblast cell at the interface. This could account for the seven non-amniotic clones in the, apparently extreme proximal, anterolateral region (Fig.1, right panel): those progenitors may have been less close to the interface than they appeared.

An additional reason for the absence of type I clones at ES stage is that four labelled descendants from the PS stage could become available to join the amniochorionic fold at MS/LS compared with only two from the ES stage.

A

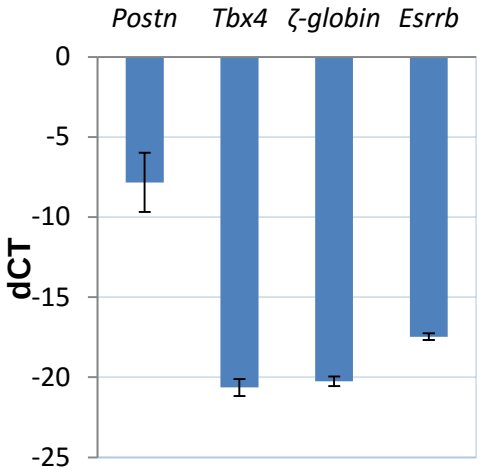

B

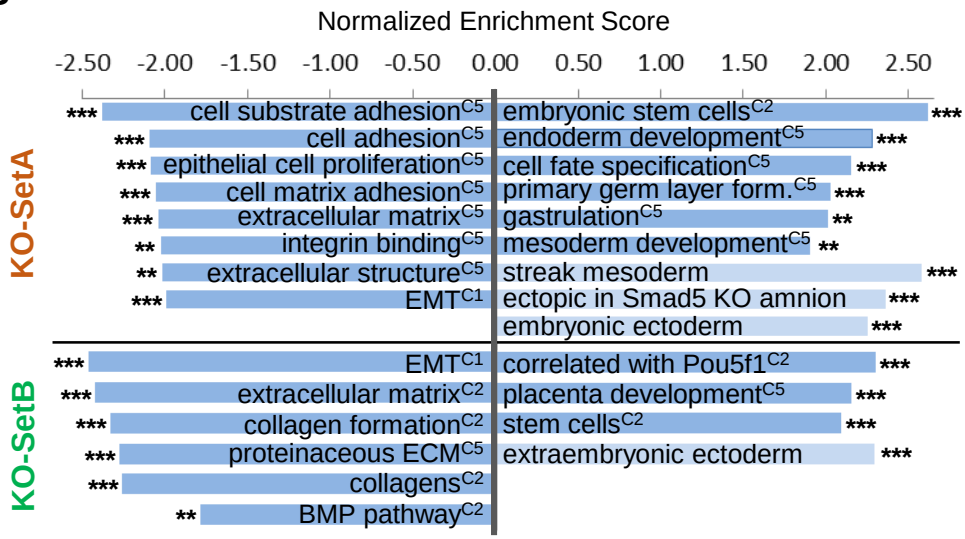

C **UNDER-expressed** **OVER-expressed**

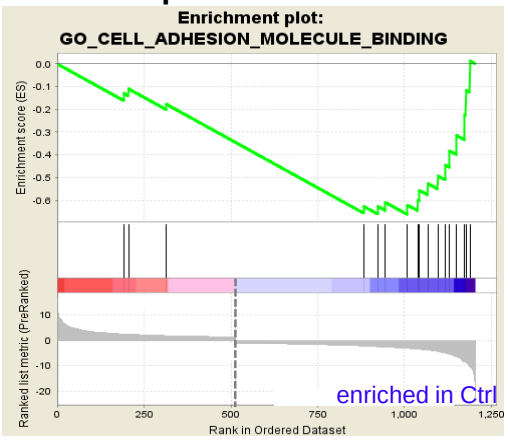

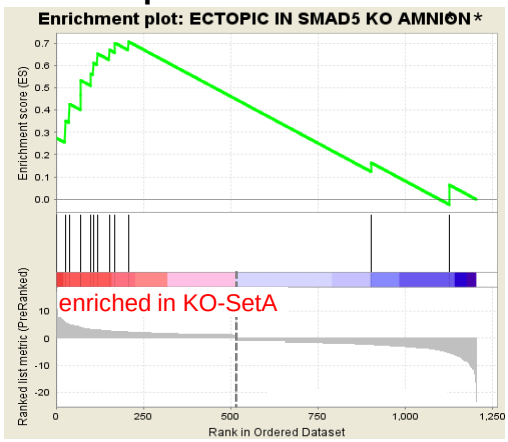

KO-SetA vs. Ctrl

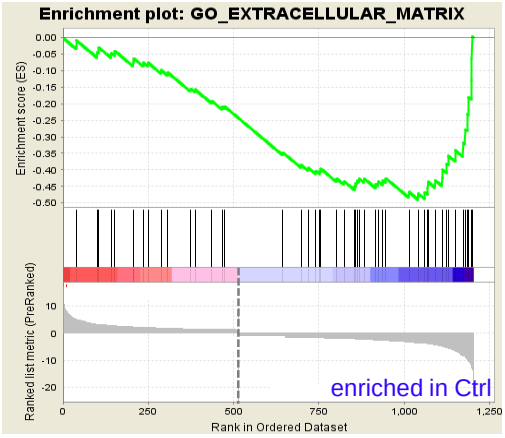

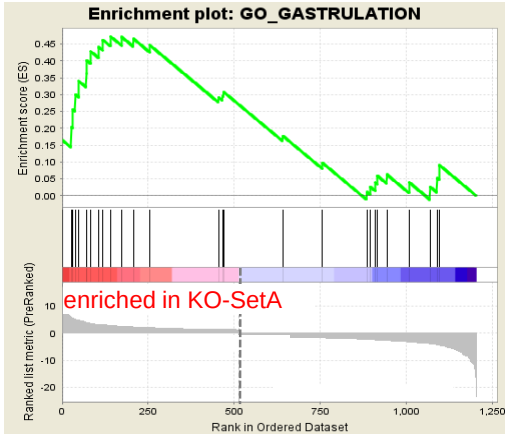

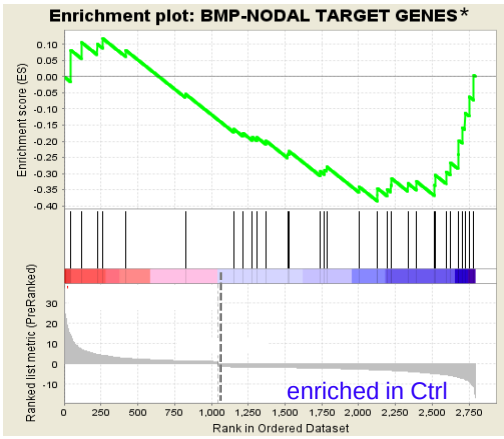

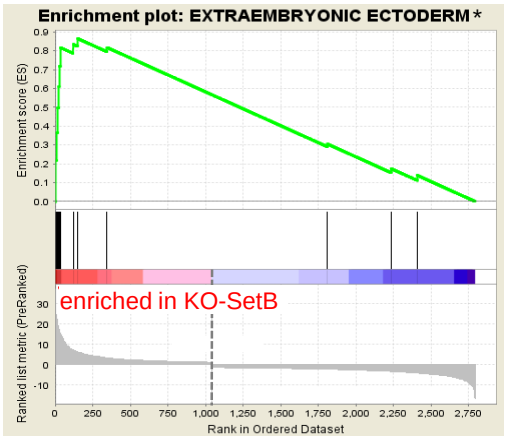

KO-SetB vs. Ctrl

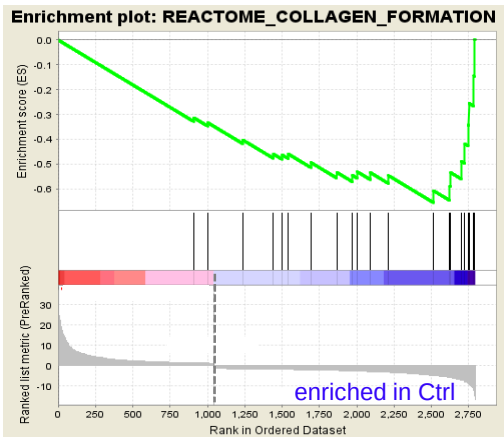

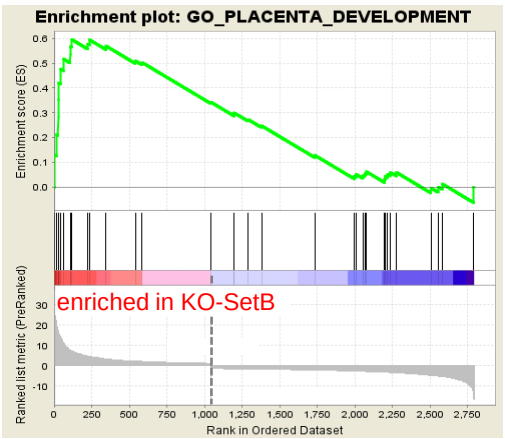

Figure S3. Analysis of differentially expressed genes shows two sets of mutants with distinct signatures

(**A**) qPCR validation of microdissected amniotic tissue. Amniotic cDNA obtained after microdissection is free from contamination with surrounding tissues, as shown by qPCR analysis for the six control amnion samples for: *Postn*, amnion marker; *Tbx4*, allantois marker; *ζ-globin*, visceral yolk sac marker; and *Esrrb*, chorion marker. KO samples were not included in the analysis due to the unknown origin of the amniotic aggregate and its streak features. For each gene, *Psmd4* normalized ΔCt values as means of the six replicates is represented, together with standard deviation (error bars).

(**B-C**) Gene set enrichment analysis (GSEAPreranked). The algorithm inquires whether a set of related genes (e.g. Gene Ontology (GO) terms) is enriched in the top or the bottom of a ranked list of transcripts (i.e. enriched in KO or Ctrl, see Supplemental Materials and Methods).

(B) A summary of selected gene sets sorted by Normalized Enrichment Score. Statistical significances: nominal p-value: ***: p<0.001, **: p<0.01, *: p<0.05.

Dark blue bars: gene sets from the Molecular Signature Database (Libertzon et al., 2011) from categories C1, C2 and C5 (see Supplemental Materials and Methods).

Light blue bars: custom-made gene sets (see Table S3). “Ectopic in Smad5 KO amnion” comprises previously reported ectopically expressed genes in the mutant amnion/aggregate (Bosman et al., 2006; Pereira et al., 2012; unpublished data).

EC - extracellular. Gene set official names, searchable on http://software.broadinstitute.org/gsea/msigdb/genesets.jsp: Enriched in KO-SetA vs Ctrl: BENPORATH_ES_1, GO_ENDODERM_DEVELOPMENT, GO_CELL_FATE_SPECIFICATION, GO_CELL_FATE_COMMITMENT_INVOLVED_IN_FORMATION_OF_PRIMARY_GERM_LAYER, GO_GASTRULATION, GO_MESODERM_DEVELOPMENT. Enriched in Ctrl vs. KO-SetA: GO_REGULATION_OF_CELL_SUBSTRATE_ADHESION, GO_POSITIVE_REGULATION_OF_CELL_ADHESION, GO_REGULATION_OF_EPITHELIAL_CELL_PROLIFERATION, GO_REGULATION_OF_CELL_MATRIX_ADHESION, GO_EXTRACELLULAR_MATRIX, GO_INTEGRIN_BINDING, GO_EXTRACELLULAR_STRUCTURE_ORGANIZATION, HALLMARK_EPITHELIAL_MESENCHYMAL_TRANSITION. Enriched in KO-SetB vs. Ctrl: KORKOLA_CORRELATED_WITH_POU5F1, GO_PLACENTA_DEVELOPMENT, CONRAD_STEM_CELL. Enriched in Ctrl vs. KO-SetB: HALLMARK_EPITHELIAL_MESENCHYMAL_TRANSITION, REACTOME_EXTRACELLULAR_MATRIX_ORGANIZATION, REACTOME_COLLAGEN_FORMATION, GO_PROTEINACEOUS_EXTRACELLULAR_MATRIX, NABA_COLLAGENS, PID_BMP_PATHWAY.

(**C**) Selected GSEAPreranked enrichment plots are shown as examples for under- and over-represented gene sets, for the comparisons KO-SetA vs. Ctrl and KO-SetB vs. Ctrl. Custom-made gene sets are marked with an asterisk, see also Table S2. The green line in the graph represents the enrichment profile, and the vertical lines are individual hits; ES – (not normalized) Enrichment Score.

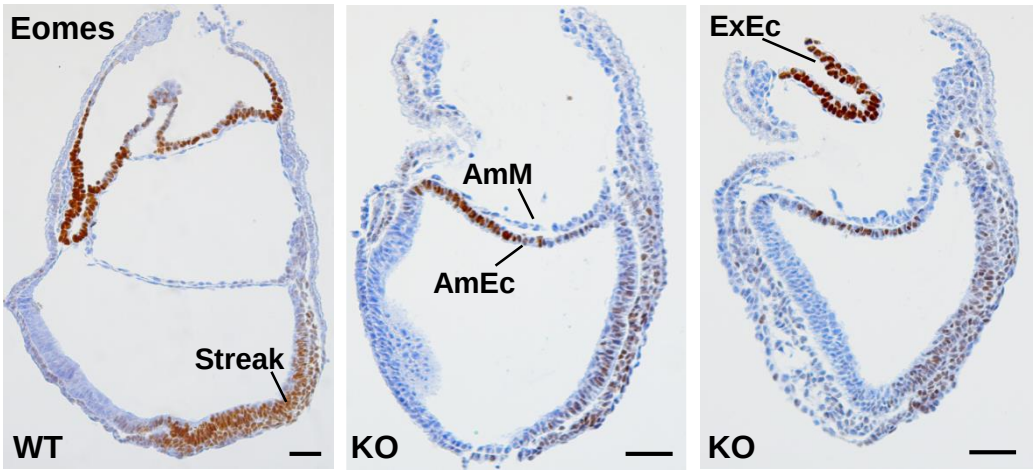

Figure S4. Localization of Eomes protein at E7.5. Immunohistochemistry on longitudinal sections of *Smad5* KO and littermate WT embryos. Eomes was detected in the streak and ExEc of both KO and WT. In KO, Eomes is also present in the amniotic ectoderm (AmEc) which is negative in the WT. The KO panels are serial sections of the same embryo. AmM – amniotic mesoderm. Scale bar: 50 µm.

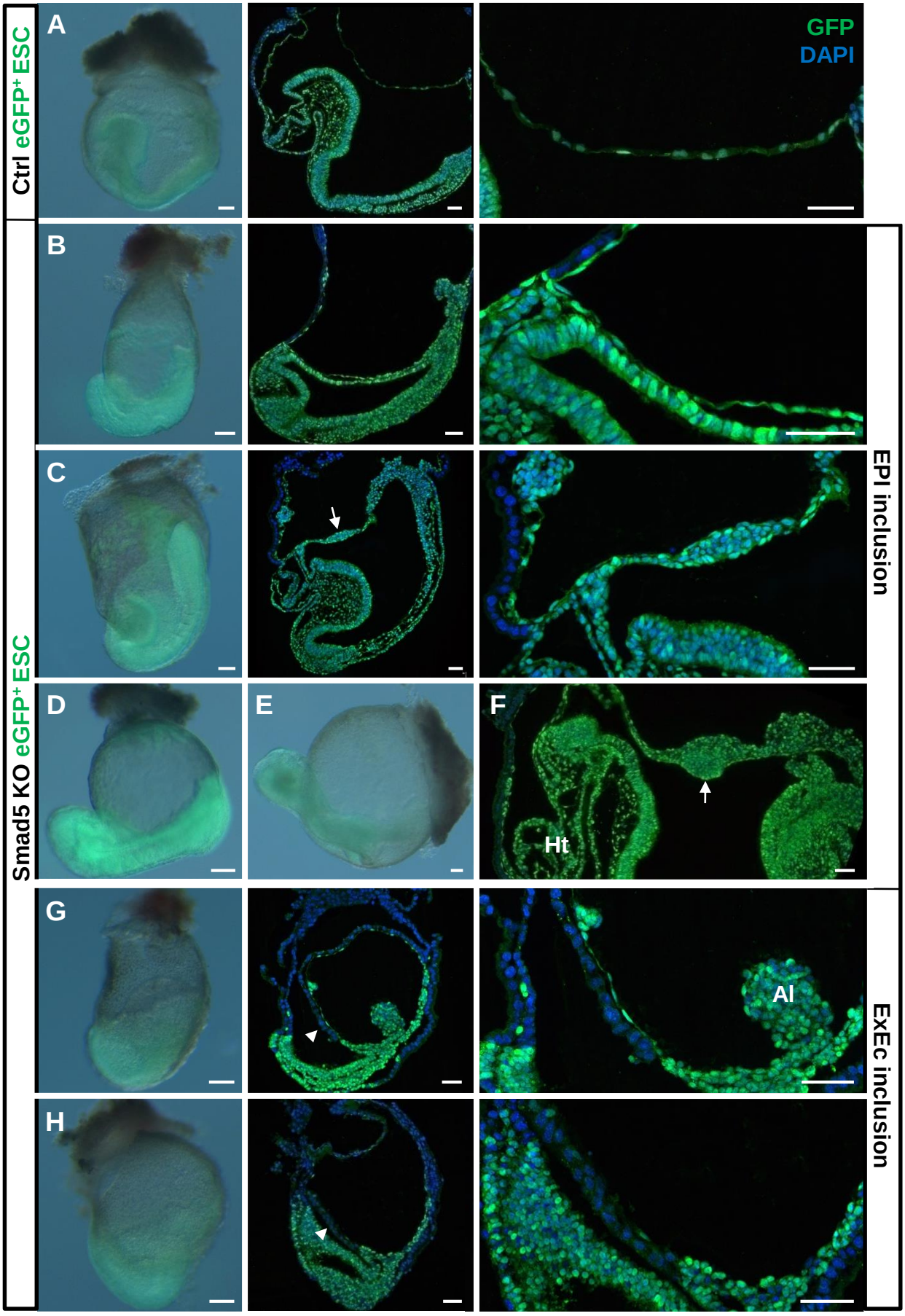

Figure S5. Amnion paucity can be compensated by different inclusion mechanisms. Whole-mount pictures of chimeric embryos derived from GFP+ WT (**A**, E8.5) or Smad5 KO ES cells (**B-E, G-H**, left panels); and longitudinal sections of the same embryos stained with anti-GFP antibody. Epiblast ectoderm (EPI) inclusion (**B-C**), as well as ExEc inclusion (**G-H**, arrowhead) were observed. Amniotic aggregates (**C**, **F**, arrows) were always GFP+ indicating their ESC/epiblast origin. Of note, some control and knockout chimeras had scattered mosaic epiblast derived tissues (Figs 7, S4, data not shown), which confirmed the observation that about half of the tetraploid acceptor embryos in a complementation setting are competent for the epiblast lineage as well (Eakin et al., 2005; Wen et al., 2014). E8.5 chimeras with extreme head-out phenotype are shown in **D** and **E**. Ht – heart; Al – allantois. Scale bars: whole mount: 100 μm, sections: 50 μm.

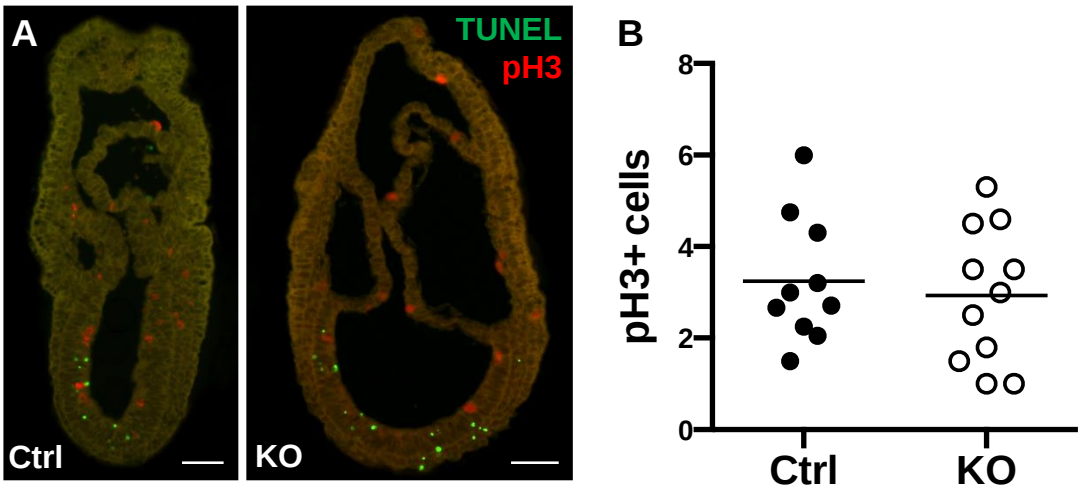

Figure S6. Proliferation and apoptosis seem unaffected in mutant amniotic ectoderm, but cell morphology and matrix proteins are disturbed in anterior amniotic ectoderm. (**A**) TUNEL assay and anti-pH3 staining in E7.0 control (n=10) and knockout (n=11) embryos before amnion-chorion separation. Negligible levels of apoptosis were detected in the amniochorionic fold (ACF). Scale bar: 50 µm.
(**B**) The average number of proliferating cells in the ectodermal component of the ACF in the same control and knockout embryos did not show significant difference (Mann-Whitney U test, p=0.69).

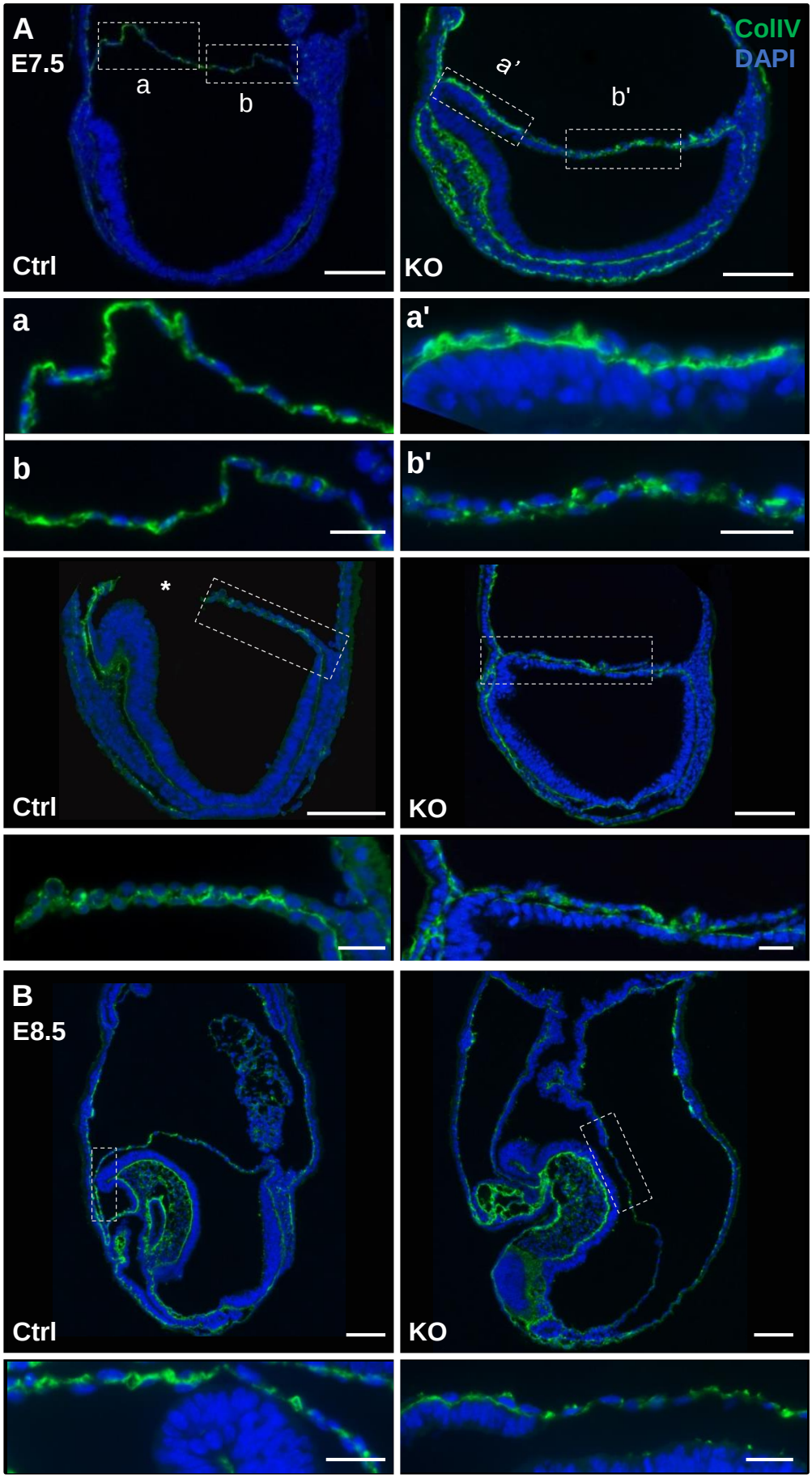

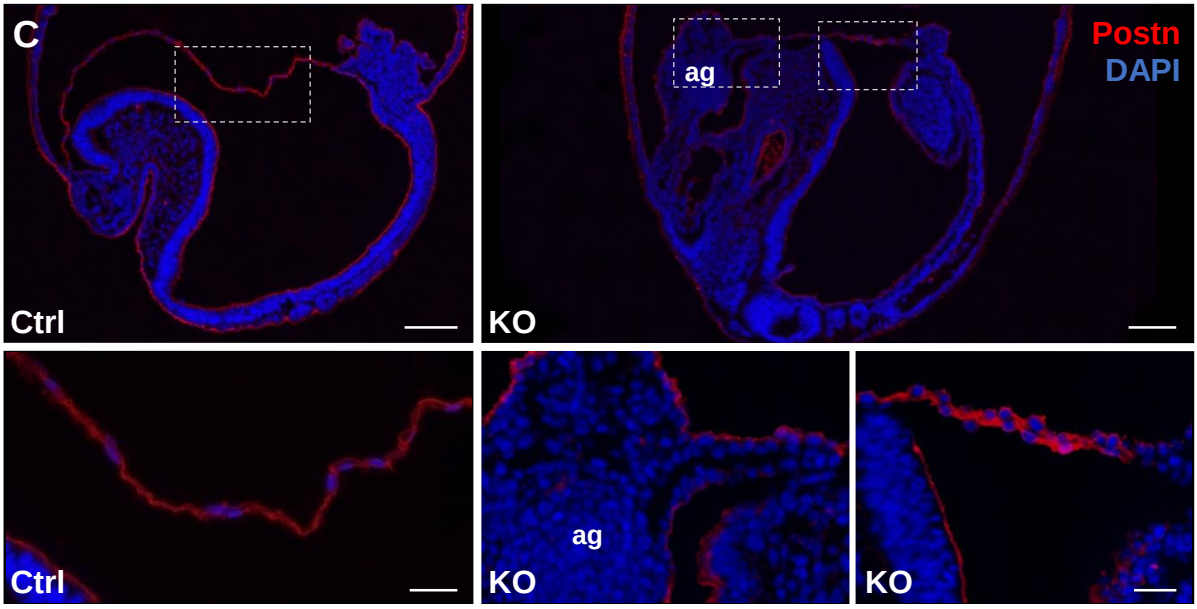

Figure S7. Antibody staining against ColIV and Postn.
Longitudinal sections of (**A**) E7.5 and (**B**) E8.5 Ctrl and Smad5 KO embryos stained agaist ColIV. In Ctrl, ColIV is distributed uniformly in the ECM between both amniotic ectoderm (AmEc) and amniotic mesoderm (AmM) cells. In knockouts, ColIV showed control-like distribution in regions of smooth amnion. In contrast, ColIV was not found between the ectodermal cells in the regions with thickened AmEc. Nuclei were stained with DAPI. Boxed area is magnified. The asterisks marks a sectioning artefact in the amnion. Scale bar: 100 µm, magnifications: 25 µm. (**C**) Localization of the amnion marker Postn (red) at E8.5. Postn is absent from the aggregate in mutants, while it is uniformly present in Ctrl amnion and in the bilayered portion of KO amnion. Nuclei are stained with DAPI (blue). Boxed area is magnified. Scale bar: 100 µm, magnifications: 25 µm.

Sample: name	type	Dev. stage	Sex	cDNA (ng)	Quality Score[1]	Input reads	% Mapping reads	Uniquely mapping reads	% Uniquely Mapped reads	% Assigned reads[2]
1.1	Ctrl	3S	♂	2175	22.96	61606749	37.8%	16394731	26.61%	88.48%
1.2	KO (SetA)	2S	♂	792	22.66	38123491	36.3%	8506141	22.31%	90.03%
2.1	Ctrl	LHF	♀	2025	22.98	49977574	38.9%	13664269	27.34%	89.21%
2.2	KO (SetB)	LHF	♀	3900	22.96	35827685	37.5%	8160168	22.78%	89.59%
3.1	Ctrl	EHF	♀	3240	22.94	44399436	37.0%	11957350	26.93%	88.10%
3.2	KO (SetA)	EHF	♀	3420	23.32	37937138	38.7%	10396617	27.40%	86.01%
4.1	Ctrl	EHF	♂	9750	23.22	33135579	38.3%	8504605	25.67%	88.77%
4.2	KO (SetB)	EHF	♀	3480	22.5	27438303	34.9%	5583741	20.35%	91.51%
5.1	Ctrl	LHF	♂	3240	23.2	40918085	38.4%	10183882	24.89%	90.07%
5.2	KO (SetB)	LPHF	♀	3690	22.7	58659608	36.3%	13600007	23.18%	90.21%
6.1	Ctrl[3]	EPHF	♂	3900	23.26	34087196	38.9%	9083874	26.65%	87.24%
6.2	KO (SetA)	EPHF	♂	3600	22.86	36364341	38.3%	9523991	26.19%	87.28%

Table S1. RNA-Seq sample details and alignment statistics.

The KO and Ctrl sample of each pair (e.g., 1.1 and 1.2) are obtained from littermates.

[1]Mean Quality Scores of the SOLiD reads per sample according to the Solexa scale (highest=40, lowest=15).

[2]uniquely mapped reads overlapping known annotated features (i.e. transcripts and exons).

[3]Sample 6.1 was initially genotyped as a control sample; however it appeared more similar to the KO samples in RNA-seq. It was excluded from further analysis.

S – somites; LHF – late headfold; EHF – early headfold; LPHF – late pre-headfold; EPHF). – early pre-headfold.

KO-SetB samples are in green, KO-SetA in orange. SetA and SetB are the categories attributed later to these samples (see text).

EMBRYONIC ECTODERM	***Fgf5, Gbx2, Fgf8, Zic3, Zic5, Six2, Zic2, Sox3, Tcfap2c, Tcfap2a,*** *Sox1, Nes, Msx2,* *Dlx5, Dlx3, Msx1, Trp63, Krt8, Krt15, Eya1, Six4, Sox2, Otx2, Six3, Hesx1, Sox1, Irx3, Foxg1, Six3, Otx2, Wnt1, Emx2, Pax6, Wnt8b, Pou3f1, Pax6, Map2, Zic1, Zic4, Sox2, Sox19, Hes1, Foxd4, Vax1, Irx2, Nkx1-2, Foxo1*
EXTRAEMBRYONIC ECTODERM	***Elf5, Cldn3, Esrrb, Sox21, Eomes, Cldn4, Sox2, Pcsk6,*** *Cited1, Bmp4, Hand1, Tcfap2a,* *Cdx2, Fgfr2, Ets2, Fgf8, Troma1, Gata3, Pl1, Pl2, Furin,*
STREAK MESODERM	***Eomes***, ***Fst***, ***T***, ***Fgf8***, ***Zic3, Mesp1, Mixl1***, ***Tbx6***, ***Lefty2***, ***Mesp2***, ***Wnt8a***, ***Evx1***, *Wnt3, Tdgf1, Cdx1, Epha2, Pdgfra, Hand1,* *Ecsit, Ext2, Hand2, Tlx2, Ext1, Foxf1a, Irx3, Lhx2, Srf, Kdr, Gsc, Lhx1, Fzd10, Hoxb1, Hoxb4, Hoxb8, Hoxa10, Cdx4, Foxh1, Foxa2, Foxc1, Foxc2, Hnf1a, Wnt3a, Wnt5a, Meox1, Lrp6, Srf, Fgf4, Fgf8, Vg1, Mixl1, Nog, Chrd, Tcf15, Pax1, Osr1, Twist1*
ECTOPIC IN SMAD5 KO AMNION	***Eomes, T, Fgf8, Mesp1, Mixl1, Lefty2, Nodal, Pou5f1, Wnt8a, Evx1, Wnt3,*** *Msx2, Fut4,* *Wnt3a, Ifitm2, Ifitm3, Alpl, Hba-x, Notch1, Gata4, Tbx2, Gsc, Foxa2, Meox1, Tcf15, Lhx1, Kdr*

Table S2. Lists of genes in each GSEA custom gene set shown in Fig. S2B. The genes enriched (core enrichment) in the top or bottom of the ranked lists of genes with cut-off p-adj. <0.05 are in bold. The genes not in bold are not enriched, and the genes in grey are not found in the ranked lists. The gene set “Ectopic in Smad5 KO amnion” contains genes previously found to be ectopically expressed in Smad5 KO amnion at mRNA or protein level (Chang et al., 1999; Bosman et al., 2006; Pereira et al., 2012; unpublished data).

	UNDER-expressed	OVER-expressed
KO-SetA vs. Ctrl		
Markers for primitive streak and streak-derived mesoderm		*Nodal, Tdgf1, Fgf8, Eomes, T, Fst, Wnt8a, Mesp1, Mesp2, Evx1, Mixl1, Tbx6*
EMT related genes		*Mmp9, Wnt3, Wnt5b*
BMP target genes and modulators	*Postn, Hand1, Hey2, Id4, Flrt3, Smoc2*	*Zic2, Zic3, Zic5*
Nodal and Nodal target genes		*Nodal, Eomes, Tdgf1 (Cripto), Lefty2, Wnt3, Fgf5, Mesp1, Mixl1*
Stem cell and PGC markers		*Pou5f1 (Oct4), Nanog, Fgf4, Tfap2c, Prdm1 (Blimp1), Prdm14*
Genes rich in amnion	*Postn, Flrt3*	
Collagens and integrins	*Col5a2, Col9a1, Col1a1, Col1a2, Col12a1, Itga4, Itga8*	
KO-SetB vs. Ctrl		
Extraembryonic ectoderm markers		*Eomes, Esrrb, Sox2, Elf5, Cldn3, Cldn4, Pcsk6, Ets2, Cited1, Sox21, Sox15*
BMP signaling components, target genes and modulators	*Bmp2, Bmp4, Smoc2, Nog, Gata4, Gata5, Gata6, Msx1, Msx2, Hand1, Hand2, Hes1, Id3, Id4, Tgfb2, Tgfbr1, Tgfbr3, Vegfa, Vegfc, Dlx2, Dlx5, Smad6, Smad1, Smad9, Smad2, Smad7, Hey2, Twist1, Twist2, Acvr1, Mmp2, Postn, Flrt3, Bmp2k, Mef2a, Cited2*	*Bmp8a, Bmp8b, Id2, Cited1, Zic5*
Genes rich in amnion	*Tfap2a*,*Twist1*,*Flrt3*	
Pluripotency-associated markers		*Dppa2, Dppa4*
Collagens and integrins	*Col9a1, Col4a5, Col5a2, Col5a1, Col1a1, Col1a2, Col4a2, Col4a1, Col4a3bp, Col23a1, Col3a1, Col4a6, Col27a1, Col26a1, Col8a2, Itga8, Itgb1*	

Table S3. Differential expression analysis highlights (cut-off: padj. <0.05).

Table S4. Top 100 most differentially expressed gense in KO-SetA or KO-SetB versus Ctrl amnion samples (RNA-Seq).

Click here to Download Table S4

A

Gene ID	Gene Name	Ctrl 1.1	Ctrl 2.1	Ctrl 3.1	Ctrl 4.1	Ctrl 5.1	KO 1.2	KO 3.2	KO 6.2	KO 2.2	KO 4.2	KO 5.2
ENSMUSG00000029337	*Fgf5*	0.0463522	0.0463522	0.2781130	0.9270433	0.0463522	5.0987380	16.2232571	9.2240805	0.0463522	0.0463522	0.0463522
ENSMUSG00000037171	*Nodal*	0.2766748	0.0553350	0.0553350	0.0553350	0.0553350	3.6521080	2.9327534	3.6521080	0.0553350	1.2727043	0.0553350
ENSMUSG00000062327	*T*	36.756044	41.212840	20.981992	104.309046	12.519089	216.480080	1006.735027	279.426057	34.051921	38.909327	26.540468
ENSMUSG00000066652	*Lefty2*	0.9767862	0.0443994	0.0443994	2.3531667	0.7547893	24.3308558	12.3430254	2.3087673	1.2431824	0.4883931	0.0443994
ENSMUSG00000027186	*Elf5*	0.0591765	0.2564315	0.1972550	0.1972550	0.3156080	0.5128630	0.1183530	0.0591765	70.8145430	42.6465298	76.6335654
ENSMUSG00000021255	*Esrrb*	0.0958548	0.1533676	0.1533676	0.0191710	0.6134705	0.3450772	0.0958548	0.0191710	39.3963110	33.9709309	39.3963110
ENSMUSG00000047501	*Cldn4*	0.3191816	0.5106906	0.0638363	0.5745269	1.0213811	0.0638363	0.8937085	0.0638363	33.0033783	24.7684928	43.2810261
ENSMUSG00000074637	*Sox2*	3.6068608	6.5374352	4.0577184	6.8755784	1.5780016	3.2687176	18.9923764	3.8322896	92.9893799	35.2232500	56.0190567
		Ctrl					KO-SetA			KO-SetB		

B

Selected genes enriched in KO-SetA

Gene ID	Comparison	log_2 Fold Change	p.adj.
Fgf5	KO-setA vs Ctrl	6.16075779794208	1.81873385913884e-10
	KO-setB vs Ctrl	-1.74310062924334	0.331548627984435
	KO-SetB vs KO-SetA	-7.90385842718541	1.23115117082365e-08
Nodal	KO-setA vs Ctrl	4.59725897942216	0.000585195595286753
	KO-setB vs Ctrl	2.17085268679028	0.16287679917155
	KO-SetB vs KO-SetA	-2.42640629263189	0.150176193285943
T	KO-setA vs Ctrl	3.58132861465481	9.12924374983415e-07
	KO-setB vs Ctrl	-0.380749064181876	0.724006771706442
	KO-SetB vs KO-SetA	-3.96207767883669	1.00111017881162e-06
Lefty2	KO-setA vs Ctrl	4.51797067858599	0.000470896168512567
	KO-setB vs Ctrl	-0.418754191923372	0.834151087607506
	KO-SetB vs KO-SetA	-4.93672487050937	0.000734872133795889

Selected genes enriched in KO-SetB

Gene ID	Comparison	log_2 Fold Change	p.adj.
Elf5	KO-setA vs Ctrl	0.279899263412563	0.880161463820885
	KO-setB vs Ctrl	8.61394649337021	1.46436300266915e-34
	KO-SetB vs KO-SetA	8.33404722995764	8.15847149665294e-25
Esrrb	KO-setA vs Ctrl	-0.0178525607789109	0.992880455772707
	KO-setB vs Ctrl	7.65968085084086	3.64140098797345e-21
	KO-SetB vs KO-SetA	7.67753341161977	6.68665855440136e-16
Cldn4	KO-setA vs Ctrl	-0.446928095611415	0.819841766795906
	KO-setB vs Ctrl	6.0755960548316	2.80619696632073e-16
	KO-SetB vs KO-SetA	6.52252415044302	1.81992898403329e-12
Sox2	KO-setA vs Ctrl	1.03108493636301	0.359532368834508
	KO-setB vs Ctrl	3.92605097755526	5.49265480860401e-08
	KO-SetB vs KO-SetA	2.89496604119225	0.00136752480201529

Table S5. Comparative analysis of selected markers representative for KO-SetA and KO-SetB *Smad5* mutant amnion. (A) Normalized expression counts (FPKM) of individual RNA-Seq samples. (B) Comparison of differential expression of the selected markers between the three groups of replicates.

Clone	Embryo identity[1]	Mouse strain	Label	h, w (μm)[2]
1	039201	B6CBA[3]	LRDX	107,153
2	149103	B6CBA	LRDX	122,138
3	169204	B6CBA	LRDX	153,168
4	169205	B6CBA	LRDX	138,153
5	149211	B6CBA	LRDX	145,145
6	149201	B6CBA	LRDX	120,130
7	379107	B6CBA	LRDX	130,138
8	149217	B6CBA	LRDX	130,122
9	279216	B6CBA	LRDX	168,168
10	279211	B6CBA	LRDX	207,199
11	269205	B6CBA	LRDX	184,168
12	279215	B6CBA	LRDX	207,184
13	240104	B6CBA	HRP/LRDX	283,245
14	439005	B6CBA	LRDX	230,214
15	468506	Dub:ICR[4]	HRP/LRDX	na
16	518607	Dub:ICR	HRP/LRDX	209,221
17	359901	B6CBA	HRP/LRDX	260,230
18	528507	Dub:ICR	HRP/LRDX	na
19	128709	Dub:ICR	HRP/LRDX	353,379
20	269208	B6CBA	LRDX	184,199
21	269202	B6CBA	LRDX	230,199
22	409008	B6CBA	LRDX	122,153
23	280805	B6CBA	HRP/LRDX	214,191
24	190812	B6CBA	HRP/LRDX	184,230
25	410101	B6CBA	HRP/LRDX	367,283
26	828608	Dub:ICR	HRP/LRDX	412,279
27	190803	B6CBA	HRP/LRDX	237,199
28	269210	B6CBA	LRDX	230,161

Table S6. List of clones.

[1]The number is a unique embryo/clone identifier. [2]Height (h) and width (w) of the embryonic portion at dissection. [3]C57BL/6 x CBA.Ca or F1 matings. [4]Dub:ICR embryos are larger than BL6CBA, but less developmentally advanced, during E6 - E7.5.

Gene	Forward primer 5' – 3'	Reverse primer 5' – 3'
RT-qPCR		
Postn	AAGGAAAAGGGTCATACACGTACTTC	CCTCTGCGAATGTCAGAATCC
Tbx4	TCAACACCTTCCCAACTCAG	GGGAGAACGGAAATAGTGATCG
ζ-globin	GCTTCAAGATCATGACCGCCGT	CGGTGGAGGCTTAGCGGTACTT
Esrrb	CCATGCACAAACTCTTCCTG	CACTTGGATCGTGTCCGTC
Gapdh	AAGAAGGTGGTGAAGCAGGC	GCCTCTCTTGCTCAGTGTCC
Psmd4	GTTCCTTCAGAGCGTCCTAG	CTATCCAACCCCGTCTTTACAG
Nodal	AAAAGTGTTGGCATCAGCCC	TGGTGCTGGCGACAGGTAC
Lefty2	TCCTTGCCCATGATTGTCAG	CTGACGAGAGCACTAAGTTAGG
T	AACAGCTCTCCAACCTATGC	TACCATTGCTCACAGACCAG
Elf5	CCGAGTGGTTAAGTCAGAAGC	CGGTGTCCATCAGAGTTTCTC
Cldn4	CCGCCAGCAACTATGTGTAAG	ACGGGCTAGTAACTTTGCAC
Sox2	GATCAGCATGTACCTCCCC	CCCTCCCAATTCCCTTGTATC
Fgf5	ACTTTCCTTCACCGTCACTG	GTATCCGAGTTTCCTTCAGGG
Sex genotyping		
Jarid1cd	CTGAAGCTTTTGGCTTTGAG	CCACTGCCAAATTCTTTGG
Sry	TGGGACTGGTGACAATTGTC	GAGTACAGGTGTGCAGCTCT
IL3	GGGACTCCAAGCTTCAATCA	TGGAGGAGGAAGAAAAGCAA
In situ hybridization		
Fgf5	ATTAACCCTCACTAAAGGGAAAACTC CATGCAAGTGCCAAA	TAATACGACTCACTATAGGGTTCC ACACGTGTAGGCACAG

Table S7. Lists of primers for RT-qPCR and sex genotyping PCR.

Supplementary Materials and Methods

Gene Set Enrichment Analyzis (GSEA).

To detect enriched functional gene sets, we ran GSEA (Subramanian et al., 2005) in PreRanked mode using the list of differentially expressed genes for each contrast (KO-SetA/Ctrl and KO-SetB/Ctrl) with padj. <0.05, ranked by the signed log of the adjusted p-value. The resulting ranked lists consisted of the genes with the "strongest" up-regulation in KO at the top of the list and the genes with the "strongest" down-regulation in KO at the bottom of the list, with the genes not changing among conditions in the middle. GSEA v.3.0 in PreRanked mode was run with the most recent version of Molecular Signatures Database (MSigDB)(Liberzon et al., 2011) – v.6.1 updated in October 2017, using the following collections of gene sets: Hallmark gene sets (Liberzon et al., 2016)(50 sets), C2 – Curated gene sets (4738 sets including Canonical pathways databases from BioCarta, KEGG and Reactome, and from expression signatures of genetic and chemical perturbations from biomedical literature), and C5 – 5917 Gene Ontology (GO) terms including all ontologies (molecular function, cellular component, and biological process)(Consortium, 2000). Gene size limits we set at 5 to 500. In addition, 4 custom made gene sets were used. Enrichment of each set of related genes in the top or bottom of the KO/ctrl ranked lists of genes was assessed by GSEA's normalized enrichment score (NES). The enrichment score reflects the degree to which a gene set is overrepresented at the top or bottom of a ranked list of genes. GSEA calculates the ES by walking down the ranked list of genes, increasing a running-sum statistic when a gene is in the gene set and decreasing it when it is not. The magnitude of the increment depends on the correlation of the gene with the phenotype. The ES is the maximum deviation from zero encountered in walking the list. A positive ES indicates gene set enrichment at the top of the ranked list; a negative ES indicates gene set enrichment at the bottom of the ranked list (Subramanian et al., 2005). The nominal p-value was used to estimate the statistical significance of the NES for each particular set.

References:

Consortium, T. G. O. (2000). Gene ontologie: Tool for the unification of biology. Nature Genetics **25**, 25–29.

Eakin, G. S., Hadjantonakis, A.-K., Papaioannou, V. E. and Behringer, **R. R.** (2005). Developmental potential and behavior of tetraploid cells in the mouse embryo. Developmental biology **288**, 150–9.

Gardner, R. L. and Cockroft, D. L. (1998). Complete dissipation of coherent clonal growth occurs before gastrulation in mouse epiblast. Development (Cambridge, England) **125**, 2397–2402.

Lawson, K. A. and Hage, W. J. (1994). Clonal analysis of the origin of primordial germ cells in the mouse. Ciba Foundation symposium **182**, 68-84-91.

Lawson, K. A., Meneses, J. J. and Pedersen, R. A. (1991). Clonal analysis of epiblast fate during germ layer formation in the mouse embryo. Development (Cambridge, England) **113**, 891–911.

McLaren, A. and Lawson, K.A. (2005). How is the mouse germ-cell lineage established? Differentiation **73,**435-7.

Liberzon, A., Subramanian, A., Pinchback, R., Thorvaldsdóttir, H., Tamayo, P. and Mesirov, J. P. (2011). Molecular signatures database (MSigDB) 3.0. Bioinformatics **27**, 1739–1740.

Liberzon, A., Birger, C., Ghandi, M., Jill, P., Tamayo, P., Jolla, L. and Jolla, L. (2016). Collection. **1**, 417–425.

Subramanian, A., Tamayo, P., Mootha, V. K., Mukherjee, S., Ebert, B. L., Gillette, M. A., Paulovich, A., Pomeroy, S. L., Golub, T. R., Lander, E. S., et al. (2005). Gene set enrichment analysis: a knowledge-based approach for interpreting genome-wide expression profiles. Proceedings of the National Academy of Sciences of the United States of America **102**, 15545–50.

Tzouanacou, E., Wegener, A., Wymeersch, F. J., Wilson, V. and Nicolas, J. F. (2009). Redefining the Progression of Lineage Segregations during Mammalian Embryogenesis by Clonal Analysis. Developmental Cell **17**, 365–376.

Wen, D., Saiz, N., Rosenwaks, Z., Hadjantonakis, A. K. and Rafii, S. (2014). Completely ES cell-derived mice produced by tetraploid complementation using inner cell mass (ICM) deficient blastocysts. PLoS ONE **9,** e94730.